optica

Subnanometer-accuracy optical distance ruler based on fluorescence quenching by transparent conductors

Robert J. Moerland[1,*] **and Jacob P. Hoogenboom**[1,2]

[1]Department of Imaging Physics, Delft University of Technology, NL-2600GA Delft, The Netherlands
[2]e-mail: j.p.hoogenboom@tudelft.nl
*Corresponding author: r.j.moerland@tudelft.nl

Transparent conductive oxides (TCOs), such as the well-known indium-tin oxide, find widespread use in modern (nano)technological applications because of their unique combination of negligible optical absorption and good electric conductivity. We, however, show that despite the near-zero imaginary part of the refractive index that is responsible for the material's transparency, TCOs drastically quench optical emitters when the emitter is within 10 nm from the TCO. Our results reveal that the pure near-field nature of this dissipation makes for an exquisite short-range optical ruler. Previous quenching-based optical rulers, based on interactions with plasmonic or graphene materials, have allowed measuring distances in the 20–100 nm range. Distances below 20 nm have, however, been hard to assess due to poor photon yields or weak absolute variations. We show that TCO-based rulers close this gap, allowing distance measurements with far-field optics in the 1–10 nm distance range with deep subnanometer sensitivity.　© 2016 Optical Society of America

OCIS codes: (180.2520) Fluorescence microscopy; (310.7005) Transparent conductive coatings; (120.2830) Height measurements.

http://dx.doi.org/10.1364/OPTICA.3.000112

1. INTRODUCTION

The behavior of quantum emitters in close proximity to metal surfaces has been extensively studied since Drexhage [1] showed how the lifetime of emitters oscillates as a function of distance to a silver mirror, and rapidly decreases for small distances, less than about 40 nm. This is due to either decay into a plasmonic mode or nonradiative transfer of energy from the emitter to the highly absorbing metal [2,3]. Both effects are included in the complex refractive index $n = n' + ik$ of the substrate [4], where n' describes the wavelength of the radiation in the material and k relates to the dissipation of optical energy by the substrate material. As a consequence, emission is effectively quenched [2,5,6] and the effective quantum yield (QY), i.e., the chance of detecting a photon in the far field, decreases. The strong dependence of the non-radiative decay rate on the distance of the emitter from the metal has been used to optically measure distances of 20–100 nm [7,8]. Similarly, quenching of fluorescence has also been reported for emitters near semiconductor interfaces [9–11], and the near-field interaction between graphene and emitters has been used for ruler applications down to 20 nm distance [12–14]. For dielectric interfaces, where $k \approx 0$, oscillations in the lifetime also occur, but less pronounced [6], and the effective QY remains constant even in close proximity. For this precise reason, dielectric substrates are unsuitable for use in quenching-based ruler applications. For indium-tin oxide (ITO), and similar transparent conductors,

$k = 2 \times 10^{-3}$ (Supplement 1, Section 1), three orders of magnitude below that of metals and semiconductors. Therefore, it is generally expected that ITO behaves similarly to, e.g., glass. Here, however, we show that such transparent conductive oxides (TCOs) show a drastic near-field fluorescence quenching at separations below the 20 nm limit of the metal and graphene rulers. In the past, Förster Resonance Energy Transfer (FRET) has been put forward as a technique to measure distances in the few-nanometer range [15]. However, in practice, FRET is used to detect conformational or "on–off" binding changes rather than measuring absolute distances, as the efficiency critically depends on the yield of the double binding of two molecules and unknown or hard-to-determine coupling factors [16]. Likewise, rulers based on detecting spectral changes in the plasmon resonances of metal nanoparticles have been successfully applied to measure distance changes of the order of a nanometer, but here also deducing absolute distances is not trivial, since a calibration of such a ruler has to be able to handle unintentional differences in the shapes and sizes of nanoparticles [17]. Instead, we will show that near-field quenching by TCOs allows distance measurements with subnanometer accuracy.

2. THEORETICAL MODEL

First, we introduce the model to calculate the normalized lifetime τ/τ_0 of emitters near a planar substrate, where τ is the lifetime of
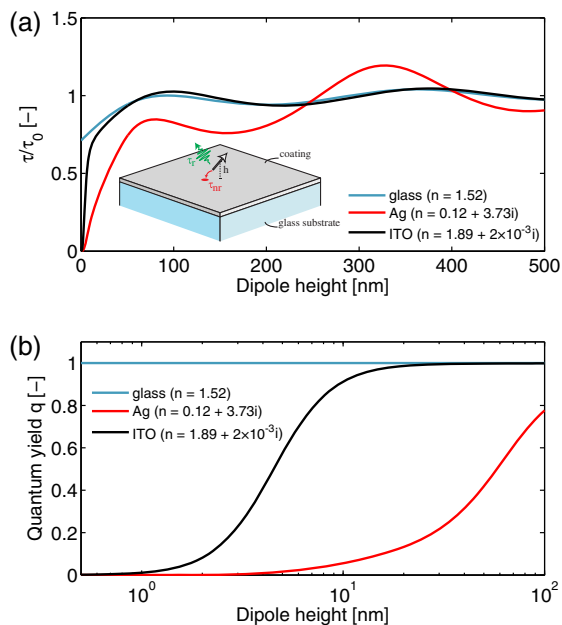
Fig. 1. Calculated lifetime and QY of a horizontally oriented emitter. (a) Lifetime as a function of distance from a bare substrate of glass, one coated with 17 nm of silver and one coated with 17 nm of ITO. The lifetime for the emitter above ITO behaves similarly to a lossless dielectric, for distances of more than 10 nm. For smaller distances, the behavior resembles that of an emitter above a metal. (b) QY of an emitter, depending on the distance from the bare glass substrate and silver- and ITO-coated substrates. The QY drops decidedly over the range from 10 nm down to 1 nm, but for a low-loss material like ITO, the QY at 1 nm (1%) still is two orders of magnitude larger than that for silver (0.01%).

the excited state in an inhomogeneous environment (e.g., near planar interfaces) and τ_0 is the excited state lifetime in a reference environment (typically vacuum). Under the assumption that the weak-coupling regime is valid such that Fermi's Golden Rule applies, the normalized lifetime, equivalent to the inverse of the relative local density of states (LDOS), can then be calculated with classical dipoles by relating [6]

$$\tau/\tau_0 = \gamma_0/\gamma = P_0/P = \text{LDOS}^{-1}, \tag{1}$$

where P and P_0 are the power emitted by a classical dipole in the inhomogeneous and reference environments, respectively. Furthermore, the decay rates in the reference and inhomogeneous environments are given by $\gamma_0 = 1/\tau_0$ and $\gamma = 1/\tau$, respectively. Then, in order to calculate the relative lifetime for a dipolar emitter near a planar interface [see the inset in Fig. 1(a) for a schematic], we use the angular spectrum representation of the dipole field [18]. This representation was used to incorporate the effect of a planar substrate on the emission of the dipole [19–21], where the substrate can have any number of additional layers, each with a different (complex) refractive index.

In Fig. 1(a), we show the calculated normalized excited state lifetime, relative to vacuum, for a horizontally [22] oriented quantum emitter as a function of the distance from an uncoated, a metal-coated, and an ITO-coated dielectric substrate. In accordance with the discussion in the introduction, the lifetime of the emitter oscillates above the dielectric, but remains finite as the emitter approaches the surface. In contrast, for a substrate

coated with 17 nm silver [23] ($k = 3.73$), the lifetime oscillations appear more pronounced, but as a major difference, the lifetime goes to 0 when the emitter approaches the substrate. This strong change lies at the base of plasmon and graphene rulers [7,12–14]. However, for these materials, the effective QY (defined as $\text{QY} = \tau_{nr}/(\tau_r + \tau_{nr})$, a ratio of nonradiative and radiative lifetimes] also drops rapidly with decreasing distance [see Fig. 1(b)], making it experimentally very challenging to measure distances below 20 nm.

Next, we turn our attention to ITO. As anticipated from the values of the refractive index, the absorbance for light at normal incidence is only about 0.1% for a 17 nm layer of ITO on glass (see Supplement 1, Section 2). Also, from Fig. 1(a), we can see that the lifetime oscillates mildly and largely in tandem with the dielectric. However, this abruptly changes for distances below 10 nm, where the lifetime is observed to drop sharply toward 0. As shown in Fig. 1(b), the QY gradually drops as the emitter gets closer to the ITO, but is larger than for the silver-based ruler. At a distance of 1 nm to the ITO, the QY of the emitter still is about 1%, whereas the QY for the silver-coated substrate has dropped to about 0.01%, two orders of magnitude lower. Therefore, only with near-transparent materials like ITO can these extremely small distances be probed reliably.

3. EXPERIMENTS

We confirm the predicted lifetime decrease on ITO experimentally, using as a proof of principle Al_2O_3 dielectric spacers created by atomic layer deposition (ALD) on ITO-coated cover glasses with an ITO thickness of 17 ± 1 nm (see also Supplement 1, Section 3). Fluorescent molecules [tetraphenoxy-perylene diimide (TPD), with peak emission at 600 nm, and Alexa Fluor 430, with peak emission at 540 nm] are dispersed onto the cover glasses at concentrations that are close to, but slightly higher than, those typically used for single-molecule studies. This way we average over a few to a few tens of molecules per measurement while avoiding self-quenching. We note that quantum dots are less suited to probe the predicted lifetime decrease because of their intrinsic size and because additional phenomena like charge transfer and photobrightening may occur simultaneously [24–26]. Fluorescence decay curves for TPD molecules for different spacer thicknesses are shown in Fig. 2. These decay curves show single-exponential decay with increasingly shorter lifetimes as the ruler distance decreases. In Fig. 3(a), the mean TPD lifetime is shown as a function of spacer thickness. The results are compared to the theoretical prediction where the effective height of the molecular transition dipole with respect to the Al_2O_3 layer is a free parameter in the model (see Supplement 1, Section 4). In this theoretical model, we explicitly include the effect that the combination of the spacer layer, the ITO layer, and the glass substrate has on the dipole emission. We find that an effective height of 1.13 ± 0.05 nm of the dipole above the Al_2O_3 layer optimally describes the measurements. The inset in Fig. 3(a) shows the measured mean fluorescence intensity as a function of spacer thickness, normalized to the predicted QY at 10 nm. At 1 nm separation, the fluorescence intensity has decreased to 2.5% of the intensity at 10 nm, but can still be recorded reliably, as also follows from Fig. 2. We note that intensity is not the preferred indicator of quantum efficiency, because experimentally it is a less rigidly defined parameter than lifetime [5]. Nevertheless, the measured dependency of fluorescence intensity on spacer thickness agrees
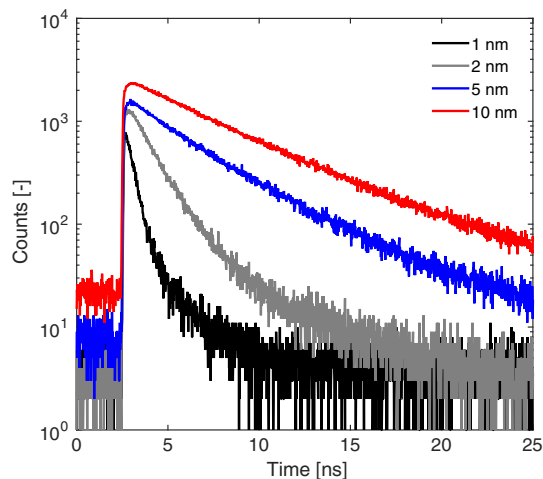
Fig. 2. Measured lifetime distributions of TPD molecules spin-coated onto ITO/glass substrates with additional alumina spacer layers of various thicknesses. Upon decreasing the thickness of the spacer layer 10-fold, the lifetime decreases by an order of magnitude.

reasonably well with predictions based on the theoretical model, using the found effective dipole distance as input. In addition, the curve illustrates the milder reduction in fluorescence signal when emitters are deposited near ITO compared with metals and graphene (see also below) [7,12–14]. A similar behavior to that of TPD, i.e., a clear lifetime reduction over a 1–10 nm distance from ITO, was observed for the commercially available fluorescent label Alexa Fluor 430. The found dependency of the lifetime on the distance is shown in Fig. 3(b), where the effective dipole distance of the emitter from the alumina layer was found to be 0.54 ± 0.05 nm (see Supplement 1, Section 5).

Our experimental results show that even the 1 nm step in spacer thickness between 1 and 2 nm is well resolved, indicating that substrates with negligible absorption could be used as sub-nanometer-accuracy optical rulers, with, in the region from about 2 to 5 nm, an approximately linear relation between lifetime and distance. In order to illustrate this, an additional data set was gathered from an extra set of TPD-coated ITO samples with Al_2O_3 spacer thicknesses ranging from 3 to 5 nm with 0.33 nm step size (three ALD cycles). The measured lifetimes as a function of spacer thickness are shown in Fig. 4. The seven data points can be clearly distinguished, and a linear fit to the data shows excellent agreement, confirming that low-absorbing transparent conductors indeed can be used as deep subnanometer optical rulers. The typical change in lifetime in this range is found to be 0.58 ± 0.05 ns/nm.

4. ORIGIN OF STRONG NEAR-FIELD QUENCHING

Our experiments clearly show the drastic lifetime reduction as a function of distance from ITO. However, with respect to the value of k for ITO (2×10^{-3}), it could be considered unexpected to see such a strong enhancement of the nonradiative decay channels. We briefly discuss the origin of this enhancement here. In Fig. 5(a), we show the power spectral density, dP/ds, of a horizontal dipole as a function of distance from the ITO. Here, s is the in-plane component of the wave vector in the plane-wave expansion after normalization with the wave vector in vacuum, i.e.,
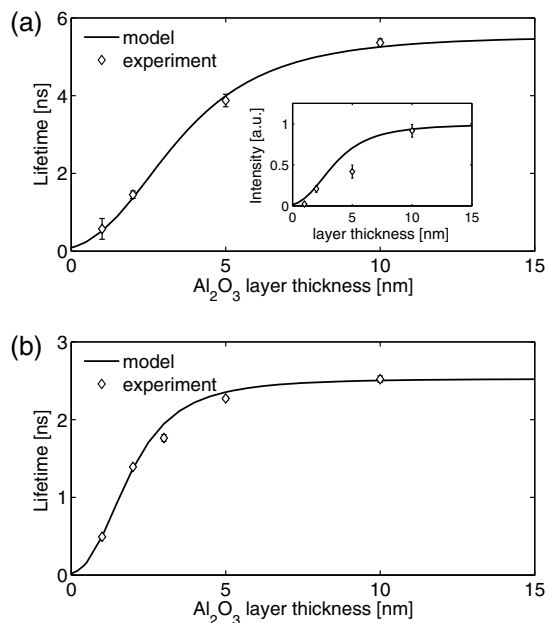

Fig. 3. Lifetime and QY reduction above an ITO-coated substrate. (a) The measured mean lifetime versus spacer thickness (diamonds). The solid curve describes the theoretical dependency of the lifetime on the spacer thickness, with a fitted typical distance of the molecules from the spacer layer of 1.13 ± 0.05 nm (see Supplement 1, Section 4). The inset displays the measured intensity (diamonds), normalized to the calculated QY (solid curve) at 10 nm. The measured intensity is 2.5% of the intensity of the fluorescence with a spacer layer of 10 nm. The error bars indicate the standard deviation in the measurements. (b) The same experiment is repeated for the commercially available fluorescent label Alexa Fluor 430. Here also the lifetime drops significantly over a distance decrease of 10 nm. The effective dipole distance from the alumina layer is 0.54 ± 0.05 nm (see Supplement 1, Section 5).
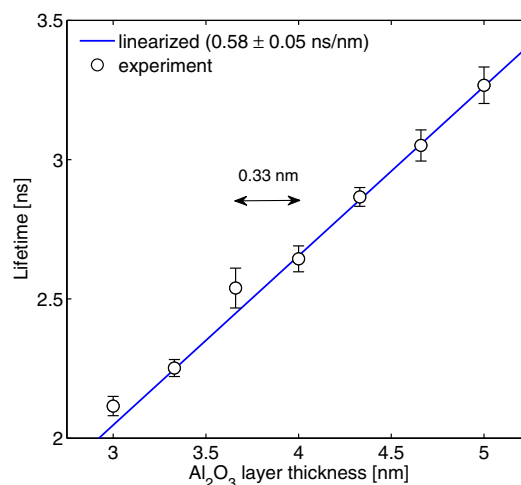

Fig. 4. Lifetime of TPD molecules as a function of layer thickness, where with each consecutive sample the spacer thickness was increased by 0.33 nm, corresponding to three ALD cycles. A linear fit, corresponding to a first-order Taylor approximation of the lifetime versus spacer thickness, agrees excellently with the data and yields a change of 0.58 ± 0.05 ns/nm. The error bars indicate the standard deviation in the measured lifetime.
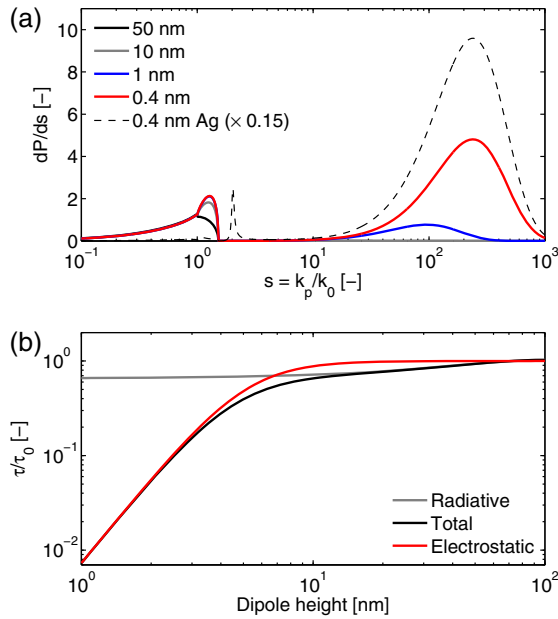
Fig. 5. (a) Power density spectrum of a horizontal dipole at four distances from a glass substrate coated with 17 nm ITO (solid curves, $\lambda = 600$ nm). The large dissipation for $s > 1.52$ and $h < 10$ nm is related to the nonpropagating part of the k-space spectrum of the dipole field. For comparison, the power density spectrum of a horizontal dipole near a 17 nm thick silver layer is shown as well (dashed curve), which indicates the presence of a surface plasmon pole around $s = 2$, absent for ITO. Moreover, strong near-field dissipation (note the scaling factor of 0.15) due to the nonpropagating part of the k-space spectrum also takes place, similarly to ITO. (b) The nonradiative part of the dipole quenching near the ITO layer is approximated well with a quasi-static description for distances smaller than about 10 nm, as the red curve shows. For comparison, the black curve is the full electromagnetic solution, and the differences are due to the radiative part (gray curve).

$s = k_{\text{parallel}}/k_0$. Then, $s = 0$ to $s = 1$ characterizes waves that can propagate both in vacuum and in the glass substrate. From $s = 1$ to $s = 1.52$, evanescent waves in the dipole field can couple into the substrate and transform into propagating waves [21]. From $s = 1.52$ and beyond, the field associated to these wave vectors cannot couple to the far field. For distances of 10 nm down to 0.4 nm, dP/ds barely changes for values of $s = 0\ldots1$. In contrast, in the range of $s = 1\ldots1.52$, evanescent waves couple more efficiently to propagating modes in the substrate with decreasing distance. Since the ITO is essentially transparent, the increase in power density in this range relates to an increase in the radiated power. However, for purely evanescent waves ($s > 1.52$), the power density increases particularly strongly [note the logarithmically scaled x axis in Fig. 5(a)]. Any dissipation at these wave vectors results in an effectively lower chance of measuring a photon in the far field. In order to compare with metals, the power spectral density for a dipole near a silver substrate is also shown in Fig. 5(a), plotted as a dashed curve. For silver substrates, coupling to surface plasmon polaritons takes place as witnessed by the peak around $s = 2$, a decay mechanism that is absent for ITO. Moreover, similarly to ITO, strong dissipation at high wave vectors (note the scaling factor of 0.15) can be seen clearly. This indicates that the mechanism behind the dissipation for $s \gg 2$ is the same for silver and ITO, but about an order of magnitude

stronger for silver, in accordance with the calculations shown in Fig. 1.

Our data point to the conclusion that the dissipation is due to the nonradiating part of the dipole field, which, despite the low losses for radiation, is still particularly strong for ITO. The waves associated with these wave vectors have been called "lossy surface waves" [5,20], but the dissipation at high wave vectors is essentially the effect of increasing Joule dissipation by the nonpropagating quasi-static part of the near field of the dipole [27], connected by a Fourier transform. Therefore, a quasi-static description should be sufficient to describe the data and the full model when dissipation in the near field is dominant. In the quasi-static approximation, the lifetime changes due to radiative rate enhancements (such as the interference of the dipole field with its own reflected field and the coupling of evanescent waves to radiative modes) are ignored. Only the direct dissipation of energy via the strong near field of the dipole in the dissipative medium is taken into account, which occurs when the two are close. In Fig. 5(b), it can be seen that this approximation describes the observed quenching well. The differences between the exact solution (black curve) and the quasi-static approximation (red curve) can be entirely attributed to changes in the radiative components of the lifetime (gray curve).

5. QUASI-TWO-DIMENSIONAL ITO LAYERS

While existing two-dimensional materials such as graphene additionally suffer from non-negligible absorption [28] ($k = 1.09i$, at $\lambda = 600$ nm, 2% absorption of radiation), thinning down the ITO to a quasi-two-dimensional, yet nonexistent, thickness of 1 nm (0.006% absorption) still shows the reported quenching. The reason behind this is that the quenching primarily occurs in the very first few tenths of a nanometer of the material, due to the overlap of the quasi-static dipole field with the ITO. Therefore, the near-field quenching is relatively insensitive to the ITO thickness, even for the nearly two-dimensional layer thicknesses. This conclusion is supported by a calculation, shown in Fig. 6, where we compare the lifetime reduction and QY of a horizontal dipole above a layer of ITO of 17 nm thickness and of 1 nm thickness, as a function of distance. The black curves in Figs. 6(a) and 6(b) represent the case where the layer is 17 nm thick, and are the same data as shown in Figs. 1(a) and 1(b), respectively, repeated for convenience. The red curve represents the case where the layer is 1 nm thick. Obviously, despite the 17 times thinner layer, the lifetime and QY show a near-identical behavior. In both cases, the experimental accessibility of the range of distances from 1 to 10 nm is superior compared with graphene (gray curve).

6. CONCLUSIONS AND DISCUSSION

We conclude that the reported distance dependency of the ITO quenching makes for an exquisite short-distance ruler with, in the 1–10 nm range, enhanced sensitivity over metal- and graphene-based quenching schemes [7,8,12–14]. This ultimate range is made accessible experimentally, thanks to the sudden onset of fluorescence quenching by ITO for very short distances. As a proof of principle, we show clearly resolved increases in lifetime that are in step with 0.33 nm increments in spacer thickness, deposited on ITO-coated glass slides. For the investigated range, this yielded a response of 0.58 ± 0.05 ns/nm.
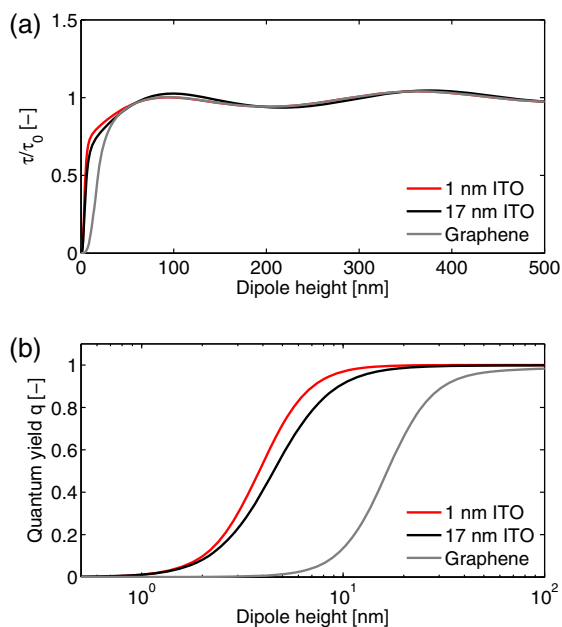
Fig. 6. Ruler performance comparison of ITO and graphene at short distances. (a) Calculated lifetime and (b) QY at $\lambda = 600$ nm of a horizontally oriented dipolar emitter versus distance from a coated glass substrate. The coatings are 1 nm of ITO (red), 17 nm of ITO (black), and a monolayer of graphene (gray). The black curve for the 17 nm thick ITO are the same data as presented in Figs. 1(a) and 1(b). Clearly, thinning the ITO coating by a factor 17 only marginally modifies the quenching behavior over all practical distances. In both cases, the experimental accessibility of the range of distances from 1 to 10 nm for nanometric ruler applications is superior compared with graphene.

The reported quenching is the result of Joule dissipation by the quasi-static near field of the emitter, which occurs by virtue of negligible absorption of radiation. Moreover, tuning the value of the complex refractive index, e.g., by optical means [29], control of the stoichiometry of the transparent conductors or by the inclusion of dopants [30], allows tuning of the distance range of the ruler. In this respect, we note that for a dielectric like BK7 glass ($k \approx 10^{-8}$), the quenching would occur below 0.1 nm, if we assume that the mathematical model would still hold at these small separations [31]. Substrate-based rulers are compatible with live-cell fluorescence measurements, including super-resolution fluorescence [8], offering distinct advantages, including robustness, over bimolecular distance rulers like with lifetime measurements in FRET [15,16]. Finally, for practical applications in areas such as solar energy conversion, plasmonics, sensing, and high-resolution microscopy, where a transparent conducting substrate may be needed, e.g., to allow electron-beam patterning or inspection, a dielectric spacer would suffice to (partially) prevent non-radiative relaxation, with 10 nm being sufficiently thick to practically recover the maximum QY.

See Supplement 1 for supporting content.

REFERENCES AND NOTES

1. K. H. Drexhage, "Influence of a dielectric interface on fluorescence decay time," J. Lumin. **1–2**, 693–701 (1970).
2. R. R. Chance, A. H. Miller, A. Prock, and R. Silbey, "Fluorescence and energy transfer near interfaces: the complete and quantitative description of the Eu^{+3}/mirror systems," J. Chem. Phys. **63**, 1589–1595 (1975).
3. I. Pockrand, A. Brillante, and D. Möbius, "Nonradiative decay of excited molecules near a metal surface," Chem. Phys. Lett. **69**, 499–504 (1980).
4. J. I. Pankove, *Optical Processes in Semiconductors* (Dover, 1971), Chap. 4, pp. 87–89.
5. W. L. Barnes, "Fluorescence near interfaces: the role of photonic mode density," J. Mod. Opt. **45**, 661–699 (1998).
6. L. Novotny and B. Hecht, *Principles of Nano-optics*, 1st ed. (Cambridge University, 2006).
7. J. Seelig, K. Leslie, A. Renn, S. Kuhn, V. Jacobsen, M. van de Corput, C. Wyman, and V. Sandoghdar, "Nanoparticle-induced fluorescence lifetime modification as nanoscopic ruler: demonstration at the single molecule level," Nano Lett. **7**, 685–689 (2007).
8. A. I. Chizhik, J. Rother, I. Gregor, A. Janshoff, and J. Enderlein, "Metal-induced energy transfer for live cell nanoscopy," Nat. Photonics **8**, 124–127 (2014).
9. T. Hayashi, T. G. Castner, and R. W. Boyd, "Quenching of molecular fluorescence near the surface of a semiconductor," Chem. Phys. Lett. **94**, 461–466 (1983).
10. A. P. Alivisatos, M. F. Arndt, S. Efrima, D. H. Waldeck, and C. B. Harris, "Electronic energy transfer at semiconductor interfaces. I. Energy transfer from two-dimensional molecular films to Si(111)," J. Chem. Phys. **86**, 6540–6549 (1987).
11. M. I. Sluch, A. G. Vitukhnovsky, and M. C. Petty, "Anomalous distance dependence of fluorescence lifetime quenched by a semiconductor," Phys. Lett. A **200**, 61–64 (1995).
12. G. Gómez-Santos and T. Stauber, "Fluorescence quenching in graphene: a fundamental ruler and evidence for transverse plasmons," Phys. Rev. B **84**, 165438 (2011).
13. L. Gaudreau, K. J. Tielrooij, G. E. Prawiroatmodjo, J. Osmond, F. J. Garcia de Abajo, and F. H. Koppens, "Universal distance-scaling of non-radiative energy transfer to graphene," Nano Lett. **13**, 2030–2035 (2013).
14. J. Tisler, T. Oeckinghaus, R. J. Stohr, R. Kolesov, R. Reuter, F. Reinhard, and J. Wrachtrup, "Single defect center scanning near-field optical microscopy on graphene," Nano Lett. **13**, 3152–3156 (2013).
15. L. Stryer and R. P. Haugland, "Energy transfer: a spectroscopic ruler," Proc. Natl. Acad. Sci. USA **58**, 719–726 (1967).
16. P. R. Selvin, "The renaissance of fluorescence resonance energy transfer," Nat. Struct. Biol. **7**, 730–734 (2000).
17. C. Sönnichsen, B. M. Reinhard, J. Liphardt, and A. P. Alivisatos, "A molecular ruler based on plasmon coupling of single gold and silver nanoparticles," Nat. Biotechnol. **23**, 741–745 (2005).
18. H. Weyl, "Ausbreitung elektromagnetischer wellen über einem ebenen leiter," Ann. Phys. **365**, 481–500 (1919).
19. W. Lukosz and R. E. Kunz, "Light-emission by magnetic and electric dipoles close to a plane interface. I. Total radiated power," J. Opt. Soc. Am. **67**, 1607–1615 (1977).
20. G. W. Ford and W. H. Weber, "Electromagnetic interactions of molecules with metal surfaces," Phys. Rep. **113**, 195–287 (1984).
21. L. Novotny, "Allowed and forbidden light in near-field optics. I. a single dipolar light source," J. Opt. Soc. Am. A **14**, 91–104 (1997).

22. We restrict ourselves to a horizontal dipole, but similar conclusions can be drawn for a vertical dipole (see Supplement 1, Section 6, and Fig. S6).
23. D. W. Lynch and W. R. Hunter, "Comments on the optical constants of metals and an introduction to the data for several metals," in *Handbook of Optical Constants of Solids*, E. D. Palik, ed. (Academic, 1997), pp. 275–367.
24. P. P. Jha and P. Guyot-Sionnest, "Electrochemical switching of the photoluminescence of single quantum dots," J. Phys. Chem. C **114**, 21138–21141 (2010).
25. S. Jin, N. Song, and T. Lian, "Suppressed blinking dynamics of single QDs on ITO," ACS Nano **4**, 1545–1552 (2010).
26. K. Patty, S. M. Sadeghi, A. Nejat, and C. B. Mao, "Enhancement of emission efficiency of colloidal CdSe quantum dots on silicon substrate via an ultra-thin layer of aluminum oxide," Nanotechnology **25**, 155701 (2014).
27. S. M. Barnett, B. Huttner, R. Loudon, and R. Matloob, "Decay of excited atoms in absorbing dielectrics," J. Phys. B **29**, 3763–3781 (1996).
28. M. Bruna and S. Borini, "Optical constants of graphene layers in the visible range," Appl. Phys. Lett. **94**, 031901 (2009).
29. M. Abb, P. Albella, J. Aizpurua, and O. L. Muskens, "All-optical control of a single plasmonic nanoantenna—ITO hybrid," Nano Lett. **11**, 2457–2463 (2011).
30. M. D. Losego, A. Y. Efremenko, C. L. Rhodes, M. G. Cerruti, S. Franzen, and J.-P. Maria, "Conductive oxide thin films: model systems for understanding and controlling surface plasmon resonance," J. Appl. Phys. **106**, 024903 (2009).
31. S. Barnett, B. Huttner, and R. Loudon, "Spontaneous emission in absorbing dielectric media," Phys. Rev. Lett. **68**, 3698–3701 (1992).